Local resonance of mechanosensitive channels

Bing Qi[a,b], Shujuan Lin[a,b], Yaohua Guo[a,b], Linglin Feng[a,b], Lijun Su[a,b], Yang Liu[c,d], Alain Goriely[c], Tian Jian Lu[a,b*], Shaobao Liu[a,b*]

[a] State Key Laboratory of Mechanics and Control for Aerospace Structures, Nanjing University of Aeronautics and Astronautics, Nanjing 210016, P.R. China

[b] MIIT Key Laboratory of Multifunctional Lightweight Materials and Structures, Nanjing University of Aeronautics and Astronautics, Nanjing 210016, P.R. China

[c] Mathematical Institute, University of Oxford, Oxford, OX2 6GG, UK

[d] Department of Mechanics, School of Mechanical Engineering, Tianjin University, Tianjin 300350, China

[*] Corresponding author: sbliu@nuaa.edu.cn, tjlu@nuaa.edu.cn

Abstract: Mechanosensitive channels are crucial biological structures that respond to mechanical stimuli by altering cellular processes. Recent studies suggest that these channels can be activated by ultrasound at specific frequencies, yet the underlying physical mechanisms remain unclear. Membrane tension is known to play a pivotal role in the regulation of mechanosensitive channels. Here, we investigate whether ultrasound can modulate membrane tension to facilitate channel activation. To do so, we develop a theoretical model based on the local resonance of mechanosensitive channels embedded in lipid membranes when subjected to ultrasonic excitation. Our results reveal that ultrasound can induce localized membrane resonance, leading to increased membrane tension in the vicinity of the channel. This tension increase, when occurring at specific resonant frequencies, is sufficient to activate mechanosensitive channels. Furthermore, we establish the effective frequency range for channel activation and examine the influence of key parameters such as ultrasound intensity, channel molecular mass, and damping effects on this range. Our findings provide a mechanistic explanation for ultrasound-induced activation of mechanosensitive channels, offering valuable insights for applications in neuromodulation, targeted therapy, and mechanomedicine.

Keywords: membrane tension, ultrasound, natural frequency, neuromodulation

1. Introduction

Mechanosensitive channels (MSCs), such as transient receptor potential (TRP) channel families, Piezo1/2, epithelial sodium channels (ENaC) (Chu et al., 2022; Douguet and Honoré, 2019), expressed across human tissues ubiquitously (Han et al., 2022; Moran et al., 2011; Raha et al., 2023; Tang et al., 2022), serve as fundamental mediators of biophysical-to-biochemical signal transduction. These molecular sensors enable sensory cells to achieve millisecond-range responsiveness to mechanical stimuli to achieve activities such as volume regulation, migration, and differentiation (Cox et al., 2019; Jin et al., 2020; Martinac, 2004). Recently, regulating MSCs through ultrasound has been considered as an effective method for neuromodulation (Duque et al., 2022; Hu et al., 2024; Ibsen et al., 2015; Kubanek et al., 2018; Oh et al., 2019; Qiu et al., 2019; Shen et al., 2021; Xian et al., 2023; Yang et al., 2021; Yoo et al., 2022), cancer treatment (Tijore et al., 2020; Wen et al., 2023), mechanoimmunology (Pan et al., 2018), reproductive improvement (Vafaie et al., 2024) and fracture repair (Zhang et al., 2021). Despite experimental evidence, the underlying mechanism by which mechanosensitive channels respond to ultrasound at specific frequencies remains unclear.

The lower frequency effects can be mostly explained by cavitation theory (Ashokkumar, 2011). For example, ultrasound at 33 kHz can activate Piezo1 channel to mediate calcium influx and potentially induce tumor cell apoptosis. However, ultrasound at 120 kHz with the same power does not work (Tijore et al., 2020). The mechanical effect caused by high-frequency ultrasound (over ~300 kHz) is more significant than cavitation effect (Thanh Nguyen et al., 2017). The mechanical effect of ultrasound is considered a physical mechanism of ultrasonic neuromodulation (Menz et al., 2019), and the majority of reported ultrasound effective frequencies that can activate mechanosensitive channels are higher than 300 kHz (see Table 1). It appears that only certain ultrasound frequencies can activate mechanosensitive channels, and the specific mechanism by which ultrasound mechanical effects act on mechanosensitive channels remains be elucidated. It is known that membrane tension plays a crucial role in the gating of mechanosensitive channels (Chu et al., 2022; Sabass and Stone, 2016; Sorum et al., 2021), even in those directly tethered to cytoskeletal or extracellular structures (Kung, 2005;

Martinac, 2014). This suggests that investigating ultrasound-induced changes in lipid membrane tension may provide insights into the activation mechanism. An ultrasonic pressure $P = \sqrt{2I\rho c}$ acting on the cell membrane may cause changes in membrane tension. The ultrasonic pressure is related to the ultrasonic intensity I, density of medium ρ and c the acoustic velocity in medium. Notably, it remains independent of ultrasound frequency. This frequency-dependent of activation is reminiscent of the resonance behavior observed in mechanical structures subjected to external excitation

Another critical aspect is the significant gap in ultrasound frequency of activating the same type mechanosensitive channels. For instance, Prieto et al. (Prieto et al., 2018) identified 43 MHz as an effective frequency for activating the Piezo1 channel, but Qiu et al. (Qiu et al., 2019) reported activation at 0.5 MHz for the same cell line (HEK293T). This discrepancy suggests that mechanosensitive channels may exhibit a spectral response mode to ultrasound, where activation occurs only within a specific frequency range. Therefore, our goal here is to determine the frequency range within which ultrasound-induced changes in membrane tension are sufficient to activate mechanosensitive channels. Additionally, we investigate how ultrasound intensity and channel parameters influence this effective frequency range.

2. Vibration of MSC under ultrasound

An MSC can be regarded as an additional mass in lipid membrane, and the stiffness of MSCs is much higher than that of the membrane (Chen et al., 2008) so that an MSC can be modelled as an oscillator inducing local resonances. Accordingly, we model the single channel structure as an MSC embedded in a local elastic circular membrane (radius a, thickness h, Young's modulus E_m, Poisson's ratio ν_m) supported by cytoskeleton network (Fig. 1 (a)). Typically, an area with radius $a < 0.007\pi R$ can approximately be regarded as a plane resting on a sphere with radius R. Based on baseline parameter values, we use $a = 200h$ in our model (details in Supplementary Information). Since the channel stiffness is ~10^5 times higher than that of lipid membrane (Chen et al., 2008; Hochmuth and Mohandas, 1972; Zhu et al., 2019), we model the channel as rigid harmonic oscillator. Similarly, the channel volume is negligible compared to

local membrane volume. When subject to periodic ultrasound, the ultrasonic force induces a deformation of the local membrane, and the inertia generated by the mass M of the channel will cause a lag in the channel position, resulting in a translational displacement δ_0 relative to the membrane (Fig. 1 (b)). Next, we derive the equation characterizing the vibration, and then extract the amplitude-frequency relation.

In the absence of viscous or forcing effect, the vibration is the result of the displacement of the oscillator in a force field. Explicitly, the translational reaction forces of MSC $F_r = F_m + F_f$ are due to both a central reaction force F_m of membrane and a force F_f due to the cytoskeletal filaments. First, the reaction force F_m generated by the central deflection δ_0 of a circular membrane with fixed boundary is (Komaragiri et al., 2005)

$$F_m = \frac{\delta_0^3 E_m h}{a^2 f^3(\nu_m)} \tag{1}$$

where $f(\nu_m) \approx 1.0491 - 0.1462\nu_m - 0.15827\nu_m^2$.

Second, we model the cytoskeletal force as a uniformly distributed load (Liu et al., 2021)

$$q = \frac{N}{4\pi R^2}\left(\frac{E_f' S_f \Delta l}{l_f} + F_0\right) \tag{2}$$

where R is the radius of a cell, N is the total number of cytoskeletal filaments in a cell, E_f', S_f, l_f, F_0 and Δl are effective Young's modulus, cross-section area, length, contraction force and virtual elastic deformation of one filament, respectively. The central deflection of circular membrane under uniformly distributed load is $\delta_0 \approx 0.823647a\left(aq/2E_m h\right)^{1/3}$ (Wei-zang et al., 1981). On the membrane, Δl is equal to δ_0, then the effective force at the center of the membrane from elastic deformation of cytoskeletal filaments under membrane reads

$$F_f = \frac{pNa^2}{R^2 f^3(\nu_m)}\left(\frac{E_f' S_f \delta_0}{l_f} + F_0\right) \tag{3}$$

where $p = 0.4118235^3\pi$. From the total reaction force $F_r = F_m + F_f$, we obtain the effective translational stiffness as

$$K = \frac{dF_r}{d\delta_0} = \frac{3E_m h\delta_0^2}{a^2 f^3(\nu_m)} + \frac{pNa^2 E_f' S_f}{R^2 l_f f^3(\nu_m)} \tag{4}$$

The parameters and their baseline values of the cytoskeletal filaments can be found in Table 2. Based on Eq. (4), for $\delta_0 < 3.1h$, the filaments dominates the vibration stiffness whereas for $\delta_0 > 3.1h$. As *a* increases, *K* tends towards a constant value. The natural angular frequency cof the system is obtained from the second term of Eq. (4), $\omega_0 = \sqrt{pNa^2 E_f' S_f / MR^2 l_f f^3(\nu_m)}$.

Including both damping and forcing, we can now write the equation for the vibration of the MSC as

$$\ddot{\delta}_0 + 2\zeta\omega_0\dot{\delta}_0 + \omega_0^2\left(\delta_0 + \varepsilon\delta_0^3\right) = B\omega_0^2\cos(\omega t + \theta) \tag{5}$$

where ζ is the damping ratio, $\varepsilon = 3E_m h / a^2 f^3(\nu_m)$ is the coefficient of nonlinear stiffness, $B = F_{ac}/M\omega_0^2$ with $F_{ac} = \pi a^2 h\rho\omega\sqrt{2I/\rho c}$ denoting the acoustic force on the membrane (Ilinskii et al., 2005; Or and Kimmel, 2009) (details in Supplementary Information), ω is the circular frequency of excitation, and θ is the phase angle. Eq. (5) takes the form of a forced-damped Duffing equation. We use the method of harmonic balance by looking for a solution of the form $\delta_0 = A_{mp}\cos(\omega t + \phi)$, and solving for A_{mp} and ϕ while neglecting higher-order harmonics. Doing so, we obtain the amplitude-frequency equation is (Nayfeh and Nook, 1979)

$$\left(\frac{B}{A_{mp}}\right)^2 - \left[1 - \left(\frac{\omega}{\omega_0}\right)^2 + \frac{3\varepsilon}{4}A_{mp}^2\right]^2 - \left(\frac{2\zeta\omega}{\omega_0}\right)^2 = 0 \tag{6}$$

The first term is generated by F_{ac}, for which *I* is the key parameter. The second term depends on the system stiffness which impedes the displacement of the MSC. It includes a constant term, $1-(\omega/\omega_0)^2$, and a nonlinear term $3\varepsilon A_{mp}^2/4$. This nonlinear behavior can induce instability in the vibration of mechanosensitive channels, where a single frequency may correspond to multiple amplitude states within certain frequency ranges, leading to abrupt amplitude transitions. The final term in the equation represents the damping effect, and we hypothesize that the damping ratio ζ may be influenced by the surface area of the channel blades. Next, we examine how the amplitude of vibration affects membrane tension to understand its variation under ultrasound excitation.

3. Membrane tension during vibration

The MSCs remain closed under the initial membrane tension σ_{r0}, while the translational displacement along the normal direction the membrane of MSC will induce a change in membrane tension. We focus our attention on the radial membrane stress of membrane rather than the circumferential stress because of the circular symmetry found in MSCs (Gandhi et al., 2011; Jiang et al., 2021; Jin et al., 2020; Tang et al., 2022). The radial membrane tension under a concentrated force F at the center is $\sigma_r = \left(9F^2Eh/\pi^2r^2\right)^{1/3}/4 + \sigma_{r0}$ (Jin, 2008), where r is the radial position. If the displacement caused by F is A_{mp}, we can use Eq. (1) to obtain the membrane tension as

$$\gamma = \frac{A_{mp}^2 hE_m}{4f^2(\nu_m)}\left(\frac{3}{\pi ra^2}\right)^{\frac{2}{3}} \tag{7}$$

Combining (6) and (7), we obtain an implicit equation for the membrane tension-frequency

$$\left[1-\left(\frac{\omega}{\omega_0}\right)^2+\frac{3\varepsilon f^2(\nu_m)\gamma}{hE_m}\left(\frac{\pi ra^2}{3}\right)^{\frac{2}{3}}\right]^2+\left(\frac{2\zeta\omega}{\omega_0}\right)^2=\frac{f^2(\nu_m)B^2hE_m}{\gamma}\left(\frac{3}{\pi ra^2}\right)^{\frac{2}{3}} \tag{8}$$

where $\gamma = \sigma_r - \sigma_{r0}$, indicating that A_{mp} causes an increase in membrane tension.

The tension γ at the channel outer wall is much larger than that at a position far away from channel (Fig. 2). The resonance response of γ showed that ultrasounds with frequencies ω around ω_0 are more likely to generate sufficient tension γ to activate the MSCs. The tension γ can change the conformation of MSC during activation by increasing the total channel area ΔA (Hamill and Martinac, 2001). The increase in conformational free energy of the channel $\gamma\Delta A > \Delta G$ indicates that γ should be sufficient to activate a channel (Turner and Sens, 2004) for typical values $\Delta A = 10\ \text{nm}^2$ (Phillips R., 2012), $\Delta G = k_B T$ (Turner and Sens, 2004), $T = 310.15$ K (Fig. 2). We conclude that the surface tension caused by ultrasound as long as their frequencies are within the *effective frequency range* that we now estimate.

4. Results and Discussions

4.1 Effective ultrasonic frequency range

The effective ultrasonic frequency range contains the frequency ω_0. Its boundaries depend on $\gamma = \Delta G/\Delta A$, with typical baseline value $\gamma = 0.428\sigma_{r0}$. From Eq. (8), we obtain the effective frequency range $[0.43\omega_0, 2.47\omega_0]$ as shown in Fig. 2.

Next, we discuss the influence of key parameters on the effective frequency range. Different types of MSCs have different molecular mass and structures, which affect M and ζ. Piezo1 with three blades has molecular mass M ~320 kDa (Li et al., 2025), while M ~220 kDa for MscL channel with five blades (Reading et al., 2015), between 32.43~182.82 kDa for TRP family with four blades (Zhang et al., 2023) and larger than 250 kDa for ASIC1 with three blades (Zha et al., 2015). Notably, the effective frequency range shrinks towards ω_0 as M increases (Fig. 3(a)). Consequently, ultrasound is more effective over a broader frequency range in activating mechanosensitive channels with lower molecular mass. This observation suggests the existence of an upper mass limit beyond which ultrasound may no longer induce channel activation. However, increasing the ultrasound intensity I can potentially raise this limit, thereby expanding the effective frequency range.

In contrast to the trend observed with increasing molecular mass M, the contraction of the effective frequency range toward ω_0 occurs more gradually as the damping ratio ζ increases. Additionally, a higher ultrasound intensity I can further expand the effective frequency range (Fig. 3(b)). The drag force influencing the vibration of mechanosensitive channels is likely attributable to interstitial fluid resistance and surface tension effects. We hypothesize that mechanosensitive channels with larger blade areas experience greater drag forces, leading to an increased damping ratio ζ, which in turn impedes their vibration.

An increase in ultrasound intensity I introduces more energy into the system, leading to a greater relative displacement between the membrane and the channel, which in turn results in a higher membrane tension γ. There exists a lower threshold of I required for the activation of mechanosensitive channels (Fig. 4), indicating that insufficient energy input is incapable of

opening the channel, a result that aligns with physical intuition. Theoretically, an infinitely high I could render all ultrasound frequencies effective for channel activation. However, excessively high ultrasound intensity poses the risk of thermal ablation of biological tissues (Hsiao et al., 2016; Zhang et al., 2015), necessitating the use of duty cycle modulation to mitigate thermal effects (Kiani et al., 2015).

The frequency range of a specific MSC can be estimated by the following method: First, we determine the membrane tension-frequency curve through Eq. (8) based on the molecular weight and other environmental parameters of different channels. Second, the critical membrane tension is calculated by changing the free energy changes ΔG and opening area ΔA, thereby determining the frequency range. The Piezo1 and MscL channels are taken as examples to reveal the difference in effective frequency ranges of channels with different values of M and ΔA (Fig. 5). In order to better demonstrate the differences between different channels, the ultrasound intensity I was taken to be 0.15 W/cm^2. Under the same excitation energy, MscL channels with less molecular mass (Li et al., 2025; Reading et al., 2015) exhibit a higher membrane amplitude. The conformational free energy change ΔG is 10 k_BT for MscL (Sukharev et al., 1994) and 50 k_BT for Piezo1 (Lin et al., 2019), while the binding area change ΔA is around 20 nm^2 for MscL (Sharma et al., 2023) and 80 nm^2 for Piezo1 (Lin et al., 2019). These values are used to determine whether the membrane amplitude is sufficient to activate the channel. The effective frequency range of MscL is broader than that of Piezo1, and the validation data is well distributed within the predicted activation frequency range as shown in Fig.5. It is emphasized that ultrasound effective frequency range will become broader with increases in the ultrasound intensity I, which is consistent with existing experimental evidence (Inoue et al., 2023).

4.2 Experiments and predictions

Many MSCs, such as Piezo1 and TRPA1 channels can be activated by quasi-static or sustainable shear and pressure (Li et al., 2014; Lüchtefeld et al., 2024; Trotier et al., 2023), which may be related to its curvature-based or tension gating in lipid membranes (Yang et al.,

2022). The changes in membrane tension caused by these lower frequency loads are more intuitive, but lower frequency external excitation is not suitable for clinical modulation due to its low targeting and resolution. Thus, we focused on the frequency range of ultrasound activated MSCs. As mentioned in the introduction, acoustic pressure is frequency independent, which is not sufficient to support the explanation of the channel's response to specific ultrasound frequencies. The resonance phenomenon is characterized by a high sensitivity to frequency, resulting in large oscillatory amplitudes that can significantly elevate local membrane tension near the channel. This observation aligns with the prevailing model of mechanosensitive channel (MSC) activation via tension gating and is applicable across various types of MSCs.

This work provides a general theoretical framework for understanding the activation of mechanosensitive channels by ultrasound at specific frequencies. The resonance model treats the mechanosensitive channel (MSC) as a particle with mass to analyze changes in membrane tension arising from local resonance under ultrasonic excitation. This theoretical framework is broadly applicable to all membrane-embedded channels. Within a biologically safe range, increasing ultrasound intensity generally facilitates channel activation; however, this effect is confined to a specific frequency range. Accordingly, our approach aims to predict the effective ultrasonic frequency range for individual channel types using Eq. (8), contingent upon preliminary studies to characterize the mechanical properties of the channel and its surrounding biophysical environment.

Validating our theoretical framework requires measuring the dynamic responses of mechanosensitive channels under ultrasound, which can be achieved through advanced microscopic imaging techniques. While this approach holds significant scientific value, it presents considerable technical challenges. Notably, many of the experimentally reported ultrasound frequencies and intensities that successfully activate channels such as Piezo1 and transient receptor potential channels fall within the predicted effective range (Fig. 4), providing preliminary support for our model. Indeed, the impact of prolonged ultrasound stimulation on channel gating remains unclear, and understanding the interplay between frequency, exposure

time, and intensity could provide deeper insights into the gating behavior of MSCs under ultrasound stimulation. We argue that in order to understand the physical mechanisms underlying ultrasound activation of force-sensitive channels, it is key to understand their frequency sensitivity is a valuable approach. Therefore, particular attention should be given to identifying frequencies that fail to activate the channels, a perspective seldom addressed in the current literature.

5. Conclusions

By investigating the frequency sensitivity of mechanosensitive channel (MSC) responses to ultrasound, we showed that channel activation can occur via a local resonance mechanism, which defines a specific effective frequency range for ultrasound-induced gating. Increased ultrasonic intensity broadens this effective range, whereas low intensity renders all frequencies ineffective. Therefore, our study provides a new direction to develop a general theoretical framework for optimizing ultrasound-based neuromodulation and targeted mechanotherapeutic strategies.

Declaration of competing interest

The authors declare that they have no known competing financial interests or personal relationships that could have appeared to influence the work reported in this paper.

Acknowledgements

This work was financially supported by the National Natural Science Foundation of China (12272179) and Jiangsu Provincial Department of Science and Technology (BK20243058).

References

Ashokkumar, M., 2011. The characterization of acoustic cavitation bubbles – An overview. Ultrason. Sonochem. 18, 864-872.

Chen, X., Cui, Q., Tang, Y., Yoo, J., Yethiraj, A., 2008. Gating Mechanisms of Mechanosensitive Channels of Large Conductance, I: A Continuum Mechanics-Based Hierarchical Framework. Biophys. J. 95, 563-580.

Chu, Y.-C., Lim, J., Chien, A., Chen, C.-C., Wang, J.-L., 2022. Activation of mechanosensitive ion channels by ultrasound. Ultrasound Med. Biol. 48, 1981-1994.

Cox, C.D., Bavi, N., Martinac, B., 2019. Biophysical Principles of Ion-Channel-Mediated Mechanosensory Transduction. Cell Rep. 29, 1-12.

Douguet, D., Honoré, E., 2019. Mammalian Mechanoelectrical Transduction: Structure and Function of Force-Gated Ion Channels. Cell 179, 340-354.

DR, L., 2008. Speed of sound in water and seawater (S = 3.5%) at different temperatures. CRC Press/Taylor and Francis, Boca Raton, FL.

Duque, M., Lee-Kubli, C.A., Tufail, Y., Magaram, U., Patel, J., Chakraborty, A., Mendoza Lopez, J., Edsinger, E., Vasan, A., Shiao, R., Weiss, C., Friend, J., Chalasani, S.H., 2022. Sonogenetic control of mammalian cells using exogenous Transient Receptor Potential A1 channels. Nat. Commun. 13, 1130.

Gandhi, C.S., Walton, T.A., Rees, D.C., 2011. OCAM: A new tool for studying the oligomeric diversity of MscL channels. Protein Sci. 20, 313-326.

Hamill, O.P., Martinac, B., 2001. Molecular basis of mechanotransduction in living cells. Physiol. Rev. 81, 685-740.

Han, D.S., Lee, C.H., Shieh, Y.D., Chang, C.T., Li, M.H., Chu, Y.C., Wang, J.L., Chang, K.V., Lin, S.H., Chen, C.C., 2022. A role for substance P and acid-sensing ion channel 1a in prolotherapy with dextrose-mediated analgesia in a mouse model of chronic muscle pain. Pain 163, e622-e633.

Hochmuth, R.M., Mohandas, N., 1972. Uniaxial loading of the red-cell membrane. J. Biomech. 5, 501-509.

Hoffman, B.U., Baba, Y., Lee, S.A., Tong, C.-K., Konofagou, E.E., Lumpkin, E.A., 2022. Focused ultrasound excites action potentials in mammalian peripheral neurons in part through the mechanically gated ion channel PIEZO2. 119, e2115821119.

Hsiao, Y.H., Kuo, S.J., Tsai, H.D., Chou, M.C., Yeh, G.P., 2016. Clinical Application of High-intensity Focused Ultrasound in Cancer Therapy. J. Cancer 7, 225-231.

Hu, H., 2000. Applied Nonlinear Dynamics. Aviation Industry Press, Beijing.

Hu, Z., Yang, Y., Yang, L., Gong, Y., Chukwu, C., Ye, D., Yue, Y., Yuan, J., Kravitz, A.V., Chen, H., 2024. Airy-beam holographic sonogenetics for advancing neuromodulation precision and flexibility. Proc. Natl. Acad. Sci. U S A 121, e2402200121.

Ibsen, S., Tong, A., Schutt, C., Esener, S., Chalasani, S.H., 2015. Sonogenetics is a non-invasive approach to activating neurons in Caenorhabditis elegans. Nat. Commun. 6, 8264.

Ilinskii, Y.A., Meegan, G.D., Zabolotskaya, E.A., Emelianov, S.Y., 2005. Gas bubble and solid sphere motion in elastic media in response to acoustic radiation force. J. Acoust. Soc. Am. 117, 2338-2346.

Inoue, S., Li, C., Hatakeyama, J., Jiang, H., Kuroki, H., Moriyama, H., 2023. Higher-intensity ultrasound accelerates fracture healing via mechanosensitive ion channel Piezo1. Bone 177, 116916.
Jiang, Y., Yang, X., Jiang, J., Xiao, B., 2021. Structural Designs and Mechanogating Mechanisms of the Mechanosensitive Piezo Channels. Trends Biochem. Sci. 46, 472-488.
Jin, C.-r., 2008. Large deflection of circular membrane under concentrated force. Appl. Math. Mech. 29, 889-896.
Jin, P., Jan, L.Y., Jan, Y.-N., 2020. Mechanosensitive Ion Channels: Structural Features Relevant to Mechanotransduction Mechanisms. Annu. Rev. Neurosci. 43, 207-229.
Kiani, H., Zhang, Z., Sun, D.W., 2015. Experimental analysis and modeling of ultrasound assisted freezing of potato spheres. Ultrason. Sonochem. 26, 321-331.
Komaragiri, U., Begley, M.R., Simmonds, J.G., 2005. The Mechanical Response of Freestanding Circular Elastic Films Under Point and Pressure Loads. J. Appl. Mech. 72, 203-212.
Kubanek, J., Shukla, P., Das, A., Baccus, S.A., Goodman, M.B., 2018. Ultrasound Elicits Behavioral Responses through Mechanical Effects on Neurons and Ion Channels in a Simple Nervous System. J. Neurosci. 38, 3081-3091.
Kung, C., 2005. A possible unifying principle for mechanosensation. Nature 436, 647-654.
Li, D., Song, Y., Zeng, Y., Hu, H., Tian, W., 2025. Research progress on PIEZO1 protein structure and activation mechanism by small-molecule agonists. Results in Chemistry 14, 102058.
Li, J., Hou, B., Tumova, S., Muraki, K., Bruns, A., Ludlow, M.J., Sedo, A., Hyman, A.J., McKeown, L., Young, R.S., Yuldasheva, N.Y., Majeed, Y., Wilson, L.A., Rode, B., Bailey, M.A., Kim, H.R., Fu, Z., Carter, D.A.L., Bilton, J., Imrie, H., Ajuh, P., Dear, T.N., Cubbon, R.M., Kearney, M.T., Prasad, K.R., Evans, P.C., Ainscough, J.F.X., Beech, D.J., 2014. Piezo1 integration of vascular architecture with physiological force. Nature 515, 279-282.
Liao, D., Li, F., Lu, D., Zhong, P., 2019. Activation of Piezo1 mechanosensitive ion channel in HEK293T cells by 30 MHz vertically deployed surface acoustic waves. Biochem. Biophys. Res. Commun. 518, 541-547.
Lim, J., Tai, H.H., Liao, W.H., Chu, Y.C., Hao, C.M., Huang, Y.C., Lee, C.H., Lin, S.S., Hsu, S., Chien, Y.C., Lai, D.M., Chen, W.S., Chen, C.C., Wang, J.L., 2021. ASIC1a is required for neuronal activation via low-intensity ultrasound stimulation in mouse brain. eLife 10, e61660.
Lin, Y.C., Guo, Y.R., Miyagi, A., Levring, J., MacKinnon, R., Scheuring, S., 2019. Force-induced conformational changes in PIEZO1. Nature 573, 230-234.
Liu, S., Yang, H., Wang, M., Tian, J., Hong, Y., Li, Y., Genin, G.M., Lu, T.J., Xu, F., 2021. Torsional and translational vibrations of a eukaryotic nucleus, and the prospect of vibrational mechanotransduction and therapy. J. Mech. Phys. Solids 155, 104572.
Liu, S., Yang, H., Xu, G.-K., Wu, J., Tao, R., Wang, M., He, R., Han, Y., Genin, G.M., Lu, T.J., Xu, F., 2024. A snap-through instability of cell adhesion under perturbations in hydrostatic pressure. J. Mech. Phys. Solids 182, 105476.
Lüchtefeld, I., Pivkin, I.V., Gardini, L., Zare-Eelanjegh, E., Gäbelein, C., Ihle, S.J., Reichmuth, A.M., Capitanio, M., Martinac, B., Zambelli, T., Vassalli, M., 2024. Dissecting cell membrane tension dynamics and its effect on Piezo1-mediated cellular mechanosensitivity using force-controlled nanopipettes. Nature Methods 21, 1063-1073.

Martinac, B., 2004. Mechanosensitive ion channels: molecules of mechanotransduction. J. Cell Sci. 117, 2449-2460.
Martinac, B., 2014. The ion channels to cytoskeleton connection as potential mechanism of mechanosensitivity. Biochim. Biophys. Acta. 1838, 682-691.
Matsushita, Y., Yoshida, K., Yoshiya, M., Shimizu, T., Tsukamoto, S., Kudo, N., Takeuchi, Y., Higuchi, M., Shimojo, M., 2024. TRPC6 is a mechanosensitive channel essential for ultrasound neuromodulation in the mammalian brain. Proc Natl Acad Sci U S A 121, e2404877121.
Menz, M.D., Ye, P., Firouzi, K., Nikoozadeh, A., Pauly, K.B., Khuri-Yakub, P., Baccus, S.A., 2019. Radiation Force as a Physical Mechanism for Ultrasonic Neurostimulation of the Ex Vivo Retina. The Journal of neuroscience : the official journal of the Society for Neuroscience 39, 6251-6264.
Moran, M.M., McAlexander, M.A., Bíró, T., Szallasi, A., 2011. Transient receptor potential channels as therapeutic targets. Nat. Rev. Drug Discov. 10, 601-620.
Nayfeh A. H. and Mook D. T. *Nonlinear Oscillations* (Wiley, 1979).
Oh, S.-J., Lee, J.M., Kim, H.-B., Lee, J., Han, S., Bae, J.Y., Hong, G.-S., Koh, W., Kwon, J., Hwang, E.-S., Woo, D.H., Youn, I., Cho, I.-J., Bae, Y.C., Lee, S., Shim, J.W., Park, J.-H., Lee, C.J., 2019. Ultrasonic Neuromodulation via Astrocytic TRPA1. Curr. Biol. 29, 3386-3401.e3388.
Or, M., Kimmel, E., 2009. Modeling Linear Vibration of Cell Nucleus in Low Intensity Ultrasound Field. Ultrasound Med. Biol. 35, 1015-1025.
Pan, Y., Yoon, S., Sun, J., Huang, Z., Lee, C., Allen, M., Wu, Y., Chang, Y.-J., Sadelain, M., Shung, K.K., Chien, S., Wang, Y., 2018. Mechanogenetics for the remote and noninvasive control of cancer immunotherapy. Proc. Natl. Acad. Sci. U S A 115, 992-997.
Phillips R., K.J., Theriot J., & Garcia H., 2012. Physical Biology of the Cell (2nd ed.). Garland Science.
Prieto, M.L., Firouzi, K., Khuri-Yakub, B.T., Maduke, M., 2018. Activation of Piezo1 but Not NaV1.2 Channels by Ultrasound at 43 MHz. Ultrasound Med. Biol. 44, 1217-1232.
Qiu, Z., Guo, J., Kala, S., Zhu, J., Xian, Q., Qiu, W., Li, G., Zhu, T., Meng, L., Zhang, R., Chan, H.C., Zheng, H., Sun, L., 2019. The Mechanosensitive Ion Channel Piezo1 Significantly Mediates In Vitro Ultrasonic Stimulation of Neurons. iScience 21, 448-457.
Raha, A., Wu, Y., Zhong, L., Raveenthiran, J., Hong, M., Taiyab, A., Wang, L., Wang, B., Geng, F., 2023. Exploring Piezo1, Piezo2, and TMEM150C in human brain tissues and their correlation with brain biomechanical characteristics. Mol. Brain 16.
Raucher, D., Sheetz, M.P., 2000. Cell spreading and lamellipodial extension rate is regulated by membrane tension. J. Cell Biol. 148, 127-136.
Reading, E., Walton, T.A., Liko, I., Marty, M.T., Laganowsky, A., Rees, D.C., Robinson, C.V., 2015. The Effect of Detergent, Temperature, and Lipid on the Oligomeric State of MscL Constructs: Insights from Mass Spectrometry. Chemistry & biology 22, 593-603.
Sabass, B., Stone, H.A., 2016. Role of the Membrane for Mechanosensing by Tethered Channels. Phys. Rev. Lett. 116, 258101.
Sharma, A., Anishkin, A., Sukharev, S., Vanegas, J.M., 2023. Tight hydrophobic core and flexible helices yield MscL with a high tension gating threshold and a membrane area mechanical strain buffer. Front Chem 11, 1159032.

Shen, X., Song, Z., Xu, E., Zhou, J., Yan, F., 2021. Sensitization of nerve cells to ultrasound stimulation through Piezo1-targeted microbubbles. Ultrason. Sonochem. 73, 105494.
Song, Y., Chen, J., Zhang, C., Xin, L., Li, Q., Liu, Y., Zhang, C., Li, S., Huang, P., 2022. Mechanosensitive channel Piezo1 induces cell apoptosis in pancreatic cancer by ultrasound with microbubbles. iScience 25.
Sorum, B., Docter, T., Panico, V., Rietmeijer, R.A., Brohawn, S.G., 2023. Pressure and ultrasound activate mechanosensitive TRAAK K⁺ channels through increased membrane tension. bioRxiv 01, 523644.
Sorum, B., Rietmeijer, R.A., Gopakumar, K., Adesnik, H., Brohawn, S.G., 2021. Ultrasound activates mechanosensitive TRAAK K(+) channels through the lipid membrane. Proc. Natl. Acad. Sci. U S A 118, e2006980118.
Sukharev, S.I., Blount, P., Martinac, B., Blattner, F.R., Kung, C., 1994. A large-conductance mechanosensitive channel in E. coli encoded by mscL alone. Nature 368, 265-268.
Tang, H., Zeng, R., He, E., Zhang, I., Ding, C., Zhang, A., 2022. Piezo-Type Mechanosensitive Ion Channel Component 1 (Piezo1): A Promising Therapeutic Target and Its Modulators. J. Med. Chem. 65, 6441-6453.
Thanh Nguyen, T., Asakura, Y., Koda, S., Yasuda, K., 2017. Dependence of cavitation, chemical effect, and mechanical effect thresholds on ultrasonic frequency. Ultrasonics Sonochemistry 39, 301-306.
Tijore, A., Margadant, F., Yao, M., Hariharan, A., Chew, C.A.Z., Powell, S., Bonney, G.K., Sheetz, M., 2020. Ultrasound-mediated mechanical forces selectively kill tumor cells. bioRxiv, 2020.2010.2009.332726.
Trotier, A., Bagnoli, E., Walski, T., Evers, J., Pugliese, E., Lowery, M., Kilcoyne, M., Fitzgerald, U., Biggs, M., 2023. Micromotion Derived Fluid Shear Stress Mediates Peri-Electrode Gliosis through Mechanosensitive Ion Channels. Adv Sci (Weinh) 10, e2301352.
Turner, M.S., Sens, P., 2004. Gating-by-tilt of mechanically sensitive membrane channels. Phys. Rev. Lett. 93, 118103.
Vafaie, A., Raveshi, M.R., Devendran, C., Nosrati, R., Neild, A., 2024. Making immotile sperm motile using high-frequency ultrasound. Sci. Adv. 10, eadk2864.
Wei-zang, C., Zhi-Zhong, W., Yin-ge, X., Shan-Lin, C., 1981. The symmetrical deformation of circular membrane under the action of uniformly distributed loads in its central portion. Appl. Math. Mech. 2, 653-668.
Wen, X., Wang, Y., Zhu, Z., Guo, S., Qian, J., Zhu, J., Yang, Z., Qiu, W., Li, G., Huang, L., Jiang, M., Tan, L., Zheng, H., Shu, Q., Li, Y., 2023. Mechanosensitive channel MscL induces non-apoptotic cell death and its suppression of tumor growth by ultrasound. Front. Chem. 11, 1130563.
Xian, Q., Qiu, Z., Murugappan, S., Kala, S., Wong, K.F., Li, D., Li, G., Jiang, Y., Wu, Y., Su, M., Hou, X., Zhu, J., Guo, J., Qiu, W., Sun, L., 2023. Modulation of deep neural circuits with sonogenetics. Proc. Natl. Acad. Sci. U S A 120, e2220575120.
Xie, K., Yang, Y., Jiang, H., 2018. Controlling Cellular Volume via Mechanical and Physical Properties of Substrate. Biophys. J. 114, 675-687.
Yang, X., Lin, C., Chen, X., Li, S., Li, X., Xiao, B., 2022. Structure deformation and curvature sensing of PIEZO1 in lipid membranes. Nature 604, 377-383.

Yang, Y., Pacia, C.P., Ye, D., Zhu, L., Baek, H., Yue, Y., Yuan, J., Miller, M.J., Cui, J., Culver, J.P., Bruchas, M.R., Chen, H., 2021. Sonothermogenetics for noninvasive and cell-type specific deep brain neuromodulation. Brain Stimul. 14, 790-800.

Ye, J., Tang, S., Meng, L., Li, X., Wen, X., Chen, S., Niu, L., Li, X., Qiu, W., Hu, H., Jiang, M., Shang, S., shu, Q., Zheng, H., Duan, S., Li, Y., 2018. Ultrasonic Control of Neural Activity through Activation of the Mechanosensitive Channel MscL. Nano Lett. 18, 4148-4155.

Yoo, S., Mittelstein, D.R., Hurt, R.C., Lacroix, J., Shapiro, M.G., 2022. Focused ultrasound excites cortical neurons via mechanosensitive calcium accumulation and ion channel amplification. Nat. Commun. 13, 493.

Zeng, Y., Yip, A.K., Teo, S.-K., Chiam, K.H., 2012. A three-dimensional random network model of the cytoskeleton and its role in mechanotransduction and nucleus deformation. Biomech. Model. Mechanobiol. 11, 49-59.

Zha, X., van Bemmelen, M.X., Huser, D., Gautschi, I., Schild, L., 2015. The Human Acid-Sensing Ion Channel ASIC1a: Evidence for a Homotetrameric Assembly State at the Cell Surface. PloS one 10, e0135191.

Zhang, G., Li, X., Wu, L., Qin, Y.-X., 2021. Piezo1 channel activation in response to mechanobiological acoustic radiation force in osteoblastic cells. Bone Res. 9, 16.

Zhang, M., Liu, L., Wang, J., Lu, K., Shu, Y., Wang, R., Liu, P., 2015. Effects of high-intensity focused ultrasound for treatment of abdominal lymph node metastasis from gastric cancer. J. Ultrasound Med. 34, 435-440.

Zhang, Y., Nie, H., Yan, X., 2023. Transient receptor potential (TRP) channels in the Manila clam (Ruditapes philippinarum): Characterization and expression patterns of the TRP gene family under heat stress in Manila clams based on genome-wide identification. Gene 854, 147112.

Zhou, W., Wang, X., Wang, K., Farooq, U., Kang, L., Niu, L., Meng, L., 2022. Ultrasound activation of mechanosensory ion channels in caenorhabditis elegans. IEEE T. Ultrason. Ferr. 69, 473-479.

Zhu, L., Cui, Q., Xiao, H., Liao, X., Chen, X., 2019. Gating and inactivation of mechanosensitive channels of small conductance: A continuum mechanics study. J. Mech. Behav. Biomed. Mater. 90, 502-514.

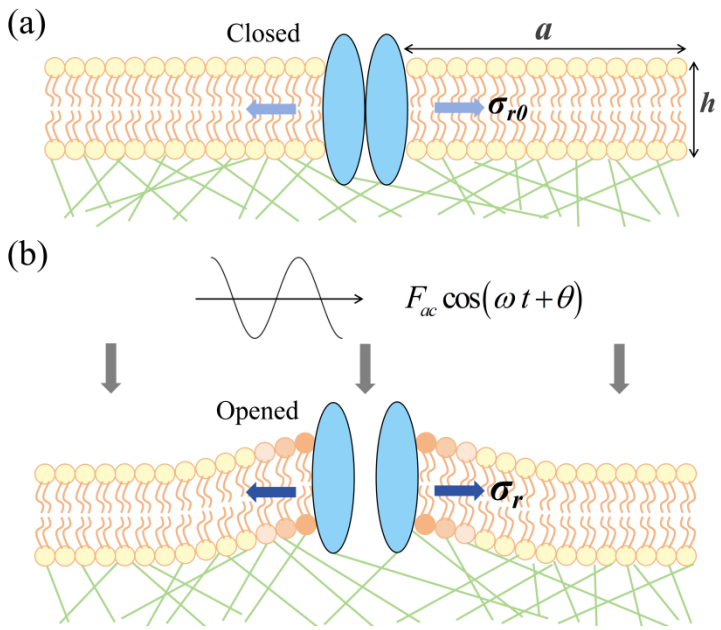

Fig. 1. Local resonance model of mechanosensitive channel. (a) One MSC embedded in local circle lipid membrane with initial membrane tension σ_{r0} supported by cytoskeleton network. (b) Periodic ultrasonic force induces deformation of local membrane, and the inertia generated by mass of the channel will cause a lag in the position change of the channel, resulting in its translational displacement relative to the membrane to change membrane tension ~~to~~ σ_r.

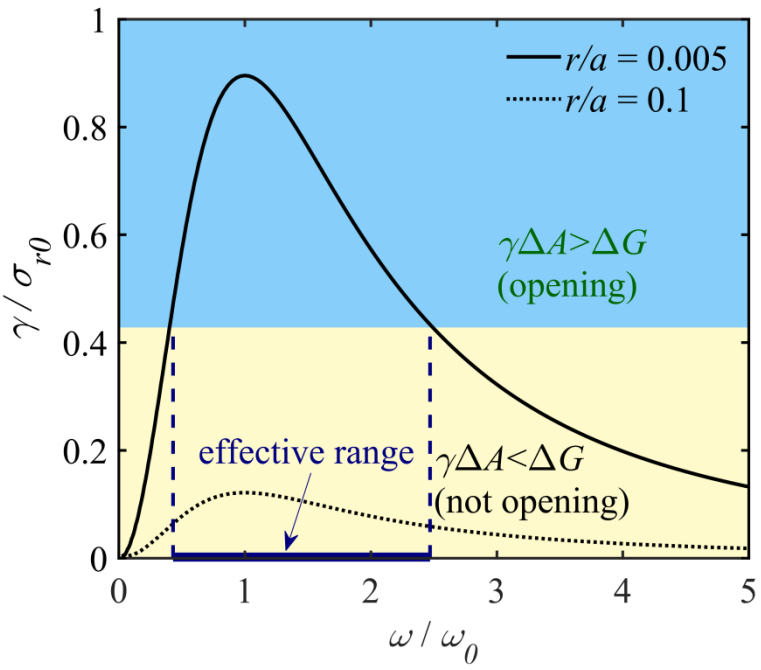

Fig. 2. Membrane tension-frequency curves. Considering an MSC with radius 1 nm, the γ at the channel outer wall (r/a = 0.005) is much higher than that of the position far away from channel, and γ caused by ultrasound within the effective frequency range makes the conformational free energy of the channel $\gamma\Delta A > \Delta G$ to activate MSCs. Baseline value I = 0.01 W/cm^2, M = 100 kDa, $\zeta = 1, \Delta A = 10$ nm^2, $\Delta G = k_B T$, T = 310.15 K, σ_{r0} = 1 mN/m.

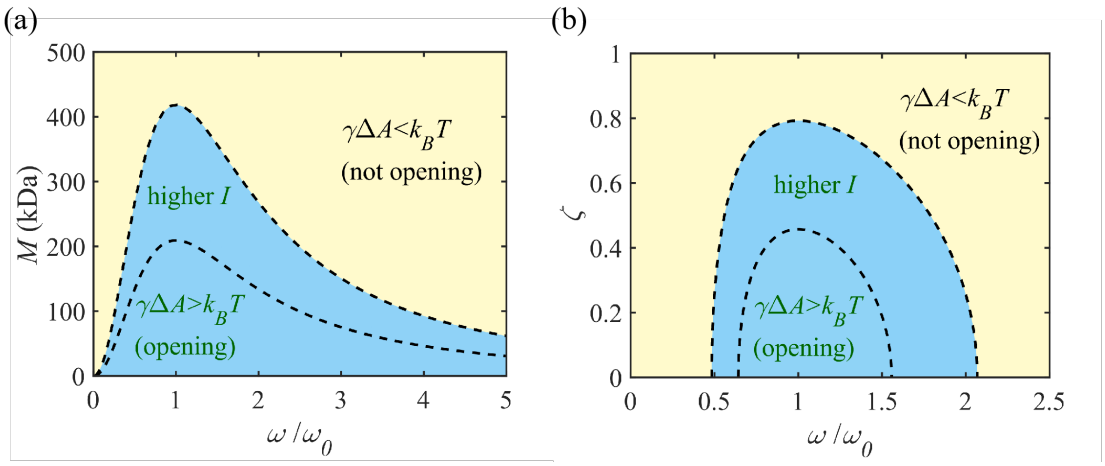

Fig. 3. Factors affecting the membrane tension. (a) The increase in membrane tension around channels with smaller molecular mass is more pronounced. $\zeta = 1$, $I = 0.01$ W/cm^2. (b) A higher damping ratio will weaken the increase in membrane tension. $M = 100$ kDa, $I = 0.001$ W/cm^2.

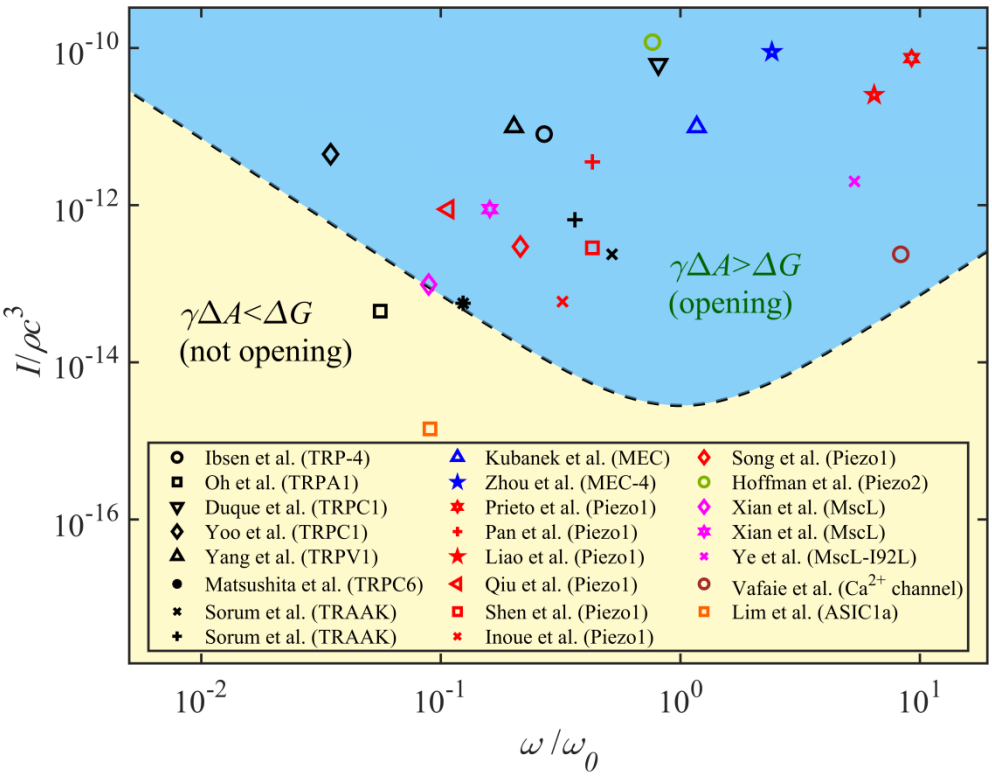

Fig. 4. Effective range of dimensional ultrasonic frequency and intensity when M = 100 kDa, ζ = 1. The experimental data (Table 1) on activation of MSCs by ultrasound are well distributed within the effective area we predicted. All frequencies have been converted to angular frequency ω in this figure.

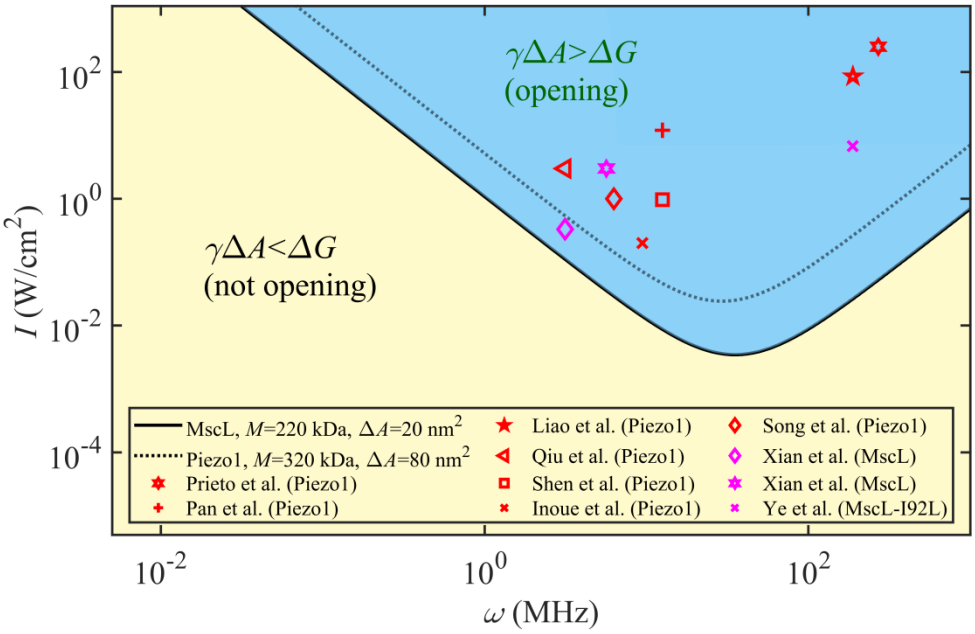

Fig. 5. The effective frequency ranges of different channels, taking MscL and Piezo1 as examples. The molecular mass M and cross-sectional area ΔA of different channels will affect the estimated effective frequency range.

Table 1 Ultrasonic intensity and frequencies for activation MSCs

MSCs types	Frequency (MHz)	Intensity (W/cm^2)
TRP-4 (Ibsen et al., 2015)	2.25	27
TRPA1 (Oh et al., 2019)	0.43	0.151
TRPC1 (Duque et al., 2022)	7	208.33
TRPC1 (Yoo et al., 2022)	0.3	15
TRPV1 (Yang et al., 2021)	1.70	33.3
TRPC6 (Matsushita et al., 2024)	1.00	0.19
TRAAK (Sorum et al., 2021)	5.00	0.8
TRAAK (Sorum et al., 2023)	3.50	2.2
MEC (Kubanek et al., 2018)	10	33.3
MEC-4 (Zhou et al., 2022)	27.4	300
Piezo1 (Prieto et al., 2018)	43	250
Piezo1 (Pan et al., 2018)	2.00	12
Piezo1 (Liao et al., 2019)	30	85.33
Piezo1 (Qiu et al., 2019)	0.5	3
Piezo1 (Shen et al., 2021)	2.00	0.963
Piezo1 (Inoue et al., 2023)	1.50	0.2
Piezo1 (Song et al., 2022)	1.00	1
Piezo2 (Hoffman et al., 2022)	3.57	400
MscL (Xian et al., 2023)	0.5	0.33
MscL (Xian et al., 2023)	0.9	3
MscL-I92L (Ye et al., 2018)	29.9	6.75
Ca^{2+} channel (Vafaie et al., 2024)	40	0.8
ASIC1a (Lim et al., 2021)	1.00	0.0048

Table 2 Parameters used in the local resonance model of MSCs vibration

Parameter	Symbol/formula	Value
The initial membrane tension	σ_{r0}	1 mN/m (Raucher and Sheetz, 2000)
Molecular mass of MSC	M	100 kDa (Gandhi et al., 2011)
Thickness of lipid membrane	h	1 nm (Xie et al., 2018)
Young's modulus of lipid membrane	E_m	6×10^5 Pa (Liu et al., 2024)
Poisson's ratio of lipid membrane	ν_m	0.33 (Liu et al., 2024)
Mass density of lipid membrane	ρ_m	1×10^3 kg (Assumed)
Radius of global membrane	R	10 μm (Liu et al., 2021)
Number of cytoskeletal filaments	N	16000 (Zeng et al., 2012)
Length of cytoskeleton filaments	l_f	10 μm (Liu et al., 2021)
Sound intensity	I	0.01 W/cm^2 (Assumed)
Acoustic velocity	c	1500 m/s (DR, 2008)
Mass density of medium	ρ	1×10^3 kg (Assumed)